Suitable Conditions for the Use of Vanadium Nitride as an Electrode for Electrochemical Capacitor

Alban Morel,[a,b,c] Yann Borjon-Piron,[a] Raúl Lucio Porto,[a,b,d,e] Thierry Brousse,[a,b,*] and Daniel Bélanger[c,*,z]

[a]*Institut des Matériaux Jean Rouxel (IMN), Université de Nantes, CNRS, 44322 Nantes Cedex 3, France*
[b]*Réseau sur le Stockage Electrochimique de l'Energie (RS2E), FR CNRS 3459, France*
[c]*Département Chimie, Université du Québec à Montréal, Succursale Centre-Ville, Montréal, Québec H3C 3P8, Canada*
[d]*Universidad Autónoma de Nuevo León, Facultad de Ingeniería Mecánica y Eléctrica, San Nicolás de los Garza, 66450 Nuevo León, México*
[e]*Universidad Autónoma de Nuevo León, Centro de Innovación, Investigación y Desarrollo en Ingeniería y Tecnología, Apodaca, 66600 Nuevo León, México*

Vanadium nitride has displayed many interesting characteristics for its use as a pseudocapacitive electrode in an electrochemical capacitor, such as good electronic conductivity, good thermal stability, high density and high specific capacitance. Thin films of VN were prepared by D.C. reactive magnetron sputtering. The electrochemical stability of the films as well as the influence of dissolved oxygen in 1 M KOH electrolyte were investigated. In order to avoid material as well as electrolyte degradation, it was concluded that vanadium nitride should only be cycled between −0.4 and −1.0 V vs. Hg/HgO. After a 24 hours stabilization period, the prepared VN thin film showed an initial capacitance of 19 mF.cm^{-2} and a capacity retention of 96% after 10000 cycles. Furthermore, dissolved oxygen in the electrolyte was demonstrated to cause self-discharge up to a potential above −0.4 V vs. Hg/HgO, where VN was shown to be unstable. Additionally, the presence of oxygen was shown to shift the open circuit potential of a VN electrode to about 0 V through self-discharge processes.

Manuscript submitted February 11, 2016; revised manuscript received March 14, 2016. Published March 29, 2016.

Electrochemical capacitors are currently being developed to complement other energy storage or conversion systems such as batteries and fuel cells. In the past two decades, several electrode materials have been investigated. The mostly studied materials include carbons,[1–8] conducting polymers[9–12] as well as pseudocapacitive[13] transition metal oxides such as ruthenium dioxide[14–18] and manganese dioxide.[19–24] In the effort to improve the performance of electrochemical capacitors, a widely used approach has been to develop synthetic methods to develop nanomaterials that are believed to lead to increased energy density and higher rate capability.[14,23,25–28]

Another approach has been to investigate the charge storage properties of novel materials. Accordingly, several research groups considered materials such as MXenes[29,30] and transition metal nitrides.[31–37] In the latter class of compounds, molybdenum nitride was firstly investigated[32,33,35,38,39] and in the past decade a great deal of attention has focused on other nitrides with an intensive focus on vanadium nitride[37,40–58] as a consequence of the impressive capacitance of 1340 F.g^{-1} reported for nanosized VN particles in 1 M KOH.[58] Indeed, VN is an interesting electrode material due to this high reported specific capacitance coupled with its close to metallic electronic conductivity (1.18 S.m^{-1}),[59] high density (6.13 g.cm^{-3}) and high melting point (2619 K).[59]

The hypothesis proposed by Choi et al.[58] to explain such a high specific capacitance of VN, is that, in addition to electrochemical double layer capacitance, successive fast reversible redox reactions are taking place, involving surface oxide groups and OH^- ions from the electrolyte. This hypothesis was supported by the observation of surface oxide via ex-situ XPS[58] and FTIR[41,58] post cycling measurements.

While most studies concentrated on new synthesis of VN with the goal to enhance the specific power density and the specific capacitance, which was found in most studies to be limited in the range of 150 to 300 F.g^{-1},[40,42–46,48–52] only few studies looked at cycling parameters-cycle life relationship. Choi et al. showed that diminishing the potential window over which the VN electrode is cycled from [−1.2; 0.0] V to [−1.2; −0.3] V vs. Hg/HgO enhanced the capacity retention after 1000 charge/discharge cycles. Further improvements were obtained when changing the electrolyte pH from 14 to 12.[58] When charging/discharging VN electrodes between −1.2 and −0.4 V instead of −1.2 and 0 V vs. Hg/HgO for 2800 cycles in 1 M KOH, Porto et al.[46] also found enhancement of the capacity retention from 0 to 70%, respectively. To our knowledge, only Lu et al.[52] studied VN over a relatively large number of charge/discharge cycles (15000 cycles). They have shown that when cycling VN up to 0.1 V vs. Hg/HgO in 1 M KOH, most of the capacitance was lost after a few thousands cycles. Interestingly, they also showed that when coating VN with carbon, the electrode kept up to 88% of its initial capacitance after 15000 cycles in 1 M KOH. All these studies highlight the need of in-depth investigations of the suitable conditions for which VN is stable as an active material for energy storage applications.

Most studies use VN powders prepared via ammonolysis of various vanadium oxides[40,42,44,45,48,49,53,60] or chloride.[37,58] As pointed out by Porto et al.,[46] this gives rise to two main drawbacks: (1) the use of different precursors especially oxides may lead to difference in compositions and especially oxygen content in the VN powders and (2) the use of powders imply the use of carbon and polymer additives in order to prepare composite electrodes, thus preventing the study of VN intrinsic electrochemical properties. On the other hand, thin film deposition techniques such as DC sputtering lead to the synthesis of VN thin films using only vanadium metal and nitrogen which can be used as-deposited as electrode material without the need of binder neither conductive additives. Additionally, tuning the deposition conditions can lead to a wide range of morphologies, from porous to dense, and to the growth of randomly or preferentially oriented thin films. Furthermore, the use of current collector is not necessary since VN thin films exhibit high electronic conductivity, and thus can be used both as active materials and current collector.

Herein, we report preparation of VN thin film working electrodes deposited on soda lime glass by D.C. sputtering and the study of their electrochemical properties by a general procedure aimed at determining the experimental conditions to obtain a stable electrode for use in an electrochemical capacitor.

*Electrochemical Society Member.
[z]E-mail: belanger.daniel@uqam.ca

Experimental

Thin film preparation.—VN thin films were prepared by D.C reactive sputtering using the AC450 sputtering system from Alliance Concept. Prior to deposition, soda lime glass substrates were degreased with successive washing with acetone and ethanol. The deposition chamber was first vacuumed to a pressure of 10^{-4} Pa. The substrates were then cleaned in situ with argon sputter etching (6 Pa, 50 sccm, 100 W RF) for 3 min. In order to ensure good adhesion of the VN thin film to the glass substrate, a titanium layer was first sputtered from a 2″ diameter titanium disk of 99.95% purity, in an argon plasma (1 Pa, 50 sccm, 50 W DC), with a target to substrate distance of 7.5 cm. The VN was then sputtered from a 2″ diameter vanadium disk of 99.5% purity, with an applied power to the target of 50 W DC, in a gas mixture of Ar/N_2 (with fixed flows of 30/2.5 sccm respectively) for a total chamber pressure of 1 Pa. Once again, the target-to-substrate distance was fixed to 7.5 cm. The deposition time was changed to control the film thickness. Unless otherwise stipulated, all prepared thin films are composed of a 140 nm thick VN layer deposited on top of a 60 nm thick titanium adhesive layer.

Thin film characterization.—The crystallographic structure of the as deposited material was investigated by X-ray diffraction with an XRD using PANalytical's X'Pert Pro diffractometer with Cu Kα radiation ($\lambda = 1.5418$ Å). Lattice parameter of the VN phase was then calculated from the refinement of the Bragg positions through the use of FullProf software. The morphological aspects of the thin films were observed using FEM-SEM Zeiss Merlin scanning electron microscope.

Electrochemical characterization.—The electrochemical properties of the thin films were investigated with a Solartron multipotentiostat 1470 coupled to a Solartron frequency analyzer 1255B. All measurements were carried out in a closed three-electrode cell with a platinum wire as counter electrode, a Hg/HgO (1 M KOH) electrode as reference electrode and a VN thin film as working electrode and current collector. For ease of reading, all potentials mentioned in the text refer to the Hg/HgO (1 M KOH) electrode potential. The cell was designed so that the VN surface area in contact with the electrolyte was limited to 0.502 cm^2 via the use of a gasket. O_2 or N_2 gas was bubbled in the aqueous 1 M KOH electrolyte for 40 min prior each experiment. In the case of experiments with N_2 gas, bubbling was also kept during the measurements. In the case of experiments with O_2 gas, the gas stream was only kept above the solution during measurements.

Prior to every EIS measurement, the electrode potential was held for 5 min at the desired potential so that the measurement would be representative of the steady state of the system. Nyquist and phase angle vs. frequency plots were then obtained by scanning the frequency from 1 kHz to 10 mHz, using a sinusoidal signal of 10 mV amplitude.

Results and Discussion

Structural characterization.—XRD patterns of a titanium adhesive layer and vanadium nitride thin film of two different thicknesses (140 and 280 nm) deposited on the titanium layer are presented in Figure 1. Comparing the XRD patterns of the samples with and without the vanadium nitride layer enables to distinguish the titanium layer diffraction peaks from those of vanadium nitride. Five diffractions peaks observed at 2Θ value of 38.0°, 44.2° 64.3°, 77.2° and 81.3° can be attributed to the vanadium nitride thin film and can be ascribed to the (111), (200), (220), (311) and (222) planes of its cubic crystal system (Fm-3m [225]), respectively. Calculation of the lattice parameter, based on the peak positions observed on the XRD pattern of the thicker VN film which presents slightly more defined peaks, results in a unit-cell parameter of $a_0 = 4.094(6)$ Å. The cell parameter for the stoichiometric bulk compound being 4.1392 Å (JCPDS file 35-768), this could reveal nitrogen vacancies in the as-deposited vanadium nitride, with a composition of $VN_{0.84}$.[61] However, a lower lattice parameter has already been reported for VN thin films prepared by D.C.

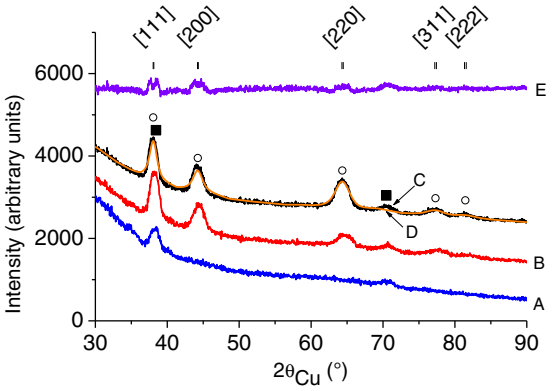

Figure 1. X-ray diffraction pattern of a 60 nm titanium adhesive layer (curve A) and of 140 (curve B) and 280 nm (Curve C) thick layer of VN on top of that adhesive layer. Curves D and E present the calculated diffraction pattern for the 280 nm thick VN layer and the difference between the measured and the calculated pattern obtained from FullProf software, respectively. The (○) and (■) symbols indicate diffraction peaks attributed to the VN and the Ti phases, respectively.

sputtering and could be explained by a compressive stress related to the deposition conditions.[62,63]

Representative SEM images of VN thin films are shown in Figure 2. The VN film exhibits columnar growth on the glass substrate (Figure 2a) with an average column diameter of 20 nm (Figure 2b). A similar morphology has been previously observed for the same type of deposition process.[46] Moreover, the irregular columnar structure observed in the cross section view (Figure 2a) as well as the observation of some pores in the top view image (Figure 2b) suggest the presence of voids in between columns.

Electrochemical characterization.—Figure 3 depicts cyclic voltammograms for Ti/VN and Ti electrodes in 1 M KOH without any nitrogen bubbling of the electrolyte. A main redox system centered at −0.67 V is observed on top of a capacitive envelope for the VN electrode. Another set of redox waves with an average potential of −1.00 V for the anodic and cathodic peak potentials is also noticed but only for the VN electrode after 20 cycles. These two redox

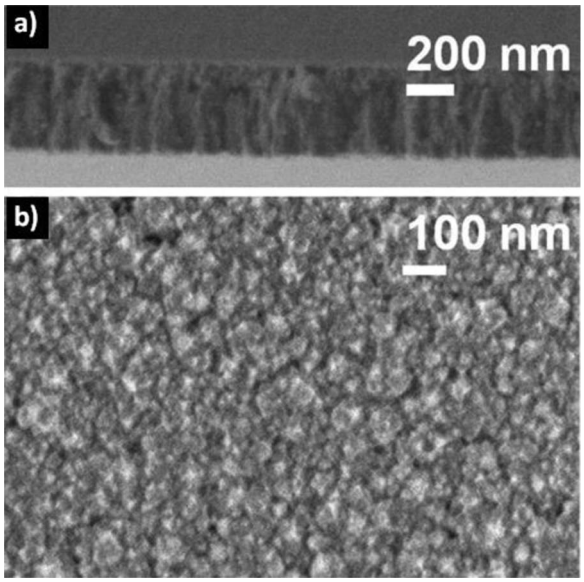

Figure 2. SEM images of a 280 nm VN/160 nm titanium bilayer thin film deposited on soda lime glass substrate a) cross section, b) top view.

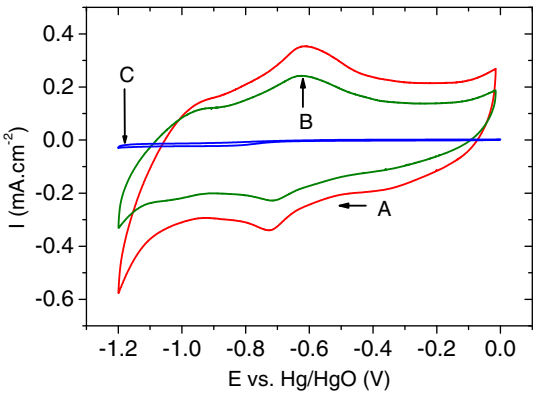

Figure 3. Cyclic voltammograms of a VN thin film (cycle #2 (curve A) and cycle #20 (curve B)) and of the adhesive titanium layer (curve C) at 20 mV.s^{-1} in non-degassed 1 M KOH electrolyte.

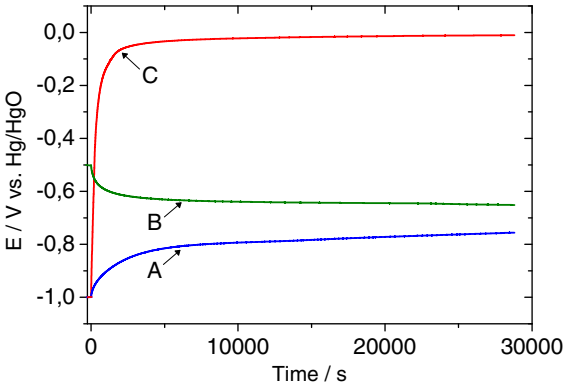

Figure 5. Open-circuit potential decay of a VN thin film following polarization at −1.0 and −0.5 V for 5 min. under N_2 (curves A and B) and O_2 (curve C) atmospheres.

systems have already been observed at similar or slightly more positive potentials.[41,43,58] Another smaller redox system centered at −0.275 V, which is not clearly observed here, is occasionally seen.[41,58] It has been suggested that these redox systems result from successive transitions from V^{+5} to V^{+2} of vanadium oxides surface sites.[58] These hypotheses have been supported by the observation of vanadium oxide by surface analysis following electrochemical cycling between 0 and −1.2 V in 1 M KOH.[41,64] However, the technical challenge that represents an in-situ investigation of such a system makes it difficult to assign each peak to a specific redox process. Moreover, the loss of electroactivity between the second and 20th cyclic voltammogram suggests that the VN thin film is not stable in these conditions. At this moment, it is difficult to explain such a loss during only 20 cycles. Figure 3 also shows an irreversible cathodic reaction for potentials more negative than −1.0 V that can be tentatively attributed to the onset of the hydrogen evolution reaction (*vide infra*). However, by decreasing the potential window (between −1.0 and −0.5 V), stable cyclic voltammograms can be obtained at 1 mV.s^{-1} (Figure 4). These conditions will then be used as starting cycling conditions in order to study the influence of oxygen dissolved in the electrolyte, prior to determine the optimal potential window over which VN electrodes could be operated. Furthermore, one can notice the negligible contribution of the titanium adhesive layer to the measured currents (Figure 3, curve C).

Influence of oxygen in the electrolyte.—Since metal nitrides are now widely investigated for water splitting (eg. the hydrogen evolution[65] and oxygen reduction reactions[66]), the effect of oxygen on the electrochemical behavior of VN was investigated. More specifically, this section aimed to emphasize and demonstrate the effect of the presence of oxygen in the electrolyte. Prior to cyclic voltammetry experiments, the electrolyte was bubbled with either N_2 or O_2 gas for 40 min. Also when N_2 was replaced by O_2, the potential of the electrode was held at −0.5 V in order to avoid any reaction that could occur if the OCP would shift to value outside of the −0.5 to −1.0 V interval. Figure 4 depicts the cyclic voltammograms obtained under N_2 and O_2. Under N_2, the CV shows a capacitive behavior and redox waves centered at −0.67 V. Anodic and cathodic charges (Q_a and Q_c, respectively) evaluated by integration of the cyclic voltammogram are very similar with values of 7.7 and 7.8 mC/cm^2, respectively. This relatively good Coulombic efficiency (99%), as well as the absence of any tail shape at the most positive and negative potential limits of the cyclic voltammogram suggest the absence of any irreversible processes. Thus, the larger cathodic charge, relative to the anodic charge, sometimes observed in the literature for VN electrodes can presumably be attributed to the presence of traces of oxygen in the electrolyte.[42,43] In contrast, only cathodic currents are observed for the cyclic voltammogram measured under O_2. This behavior reveals the irreversible oxygen reduction reaction due to presence of oxygen in the solution (Eq. 1). Bubbling oxygen in the electrolyte was performed only to emphasize the electrochemical response of this reaction on a VN electrode. However, one should realize that such irreversible reaction will contribute a cathodic charge (eg. in the presence of traces of oxygen) that will counterbalance and hide the effect of any irreversible anodic process, when evaluating the Coulombic efficiency.

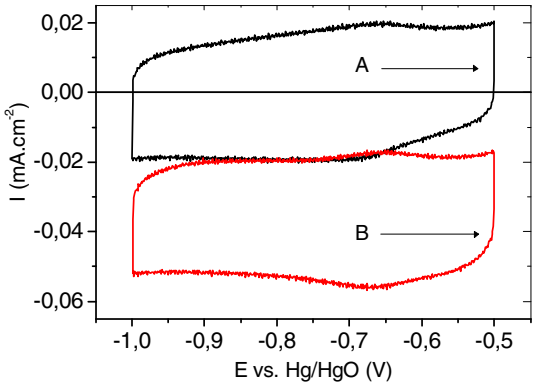

Figure 4. Cyclic voltammograms of a VN thin film under N_2 (curve A) and O_2 (curve B) atmospheres at 1 mV.s^{-1} in 1 M KOH.

$$O_2 + 2H_2O + 4e^- \leftrightarrows 4OH^- \quad [1]$$

The influence of oxygen can also be observed when comparing the evolution of the open-circuit potential (OCP) of the electrode in presence of N_2 and O_2 (Figure 5). In this experiment, the electrode potential was firstly cycled between −0.5 and −1.0 V and polarized at either −1.0 or −0.5 V prior to monitoring the evolution of the OCP for 8 hours. The measurements made under nitrogen show a slow decay/recovery of the thin film OCP from −1.00 to −0.76 V and −0.50 to −0.65 V. On the other hand, in the presence of oxygen, a very fast decay of potential is observed and reached −0.10 V in less than 25 min and −0.01 V after 8 hours regardless of the initial potential. This drastic self-discharge is another example of the influence of the oxygen reduction reaction (Eq. 1) taking place at the electrode until its potential reaches the equilibrium potential of that reaction (E° = 0.298 V vs. Hg/HgO (1 M KOH)), or until an equilibrium is reached between this reduction reaction and an oxidation reaction (e.g., corrosion process through oxidation of the material and reduction of oxygen). Following an additional 24 hours immersion in presence of oxygen, the degradation of the thin film was visually observed. The fact that the OCP does not reach 0.298 V and that degradation is observed corroborate the hypothesis of a corrosion process in presence of oxygen. Moreover, a significant corrosion rate has been reported for VN in NaOH at 80°C.[67]

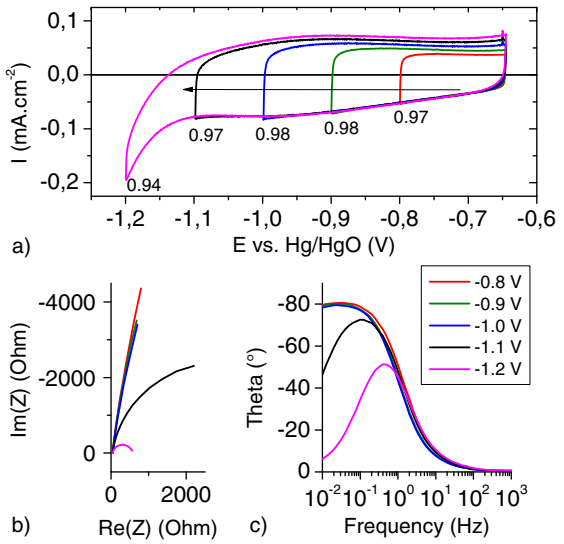

Figure 6. a) Cyclic voltammograms of VN thin film electrode between its open circuit potential and various more negative potential limits. The values at each lower potential limit represent the ratio of anodic and cathodic charge (Qa/Qc). b) Nyquist plots (1 kHz - 10 mHz) and c) Bode plots measured by electrochemical impedance spectroscopy at these various negative potential limits. Measurements made in 1 M KOH under N_2 atmosphere.

It can be noted that the methodology used here can be applied to the investigation of any new electrode material for electrochemical capacitor. In summary, when investigating a material as an electrode for energy storage applications and when oxygen is present in the electrolyte, the irreversible oxygen reduction reaction can take place. In a charge/discharge cycle, the cathodic charge consumed by such irreversible reduction reaction could hide or minimize the presence of an irreversible oxidation reaction. This could result in a capacity loss due to oxidation/dissolution or passivation of the material even though the Coulombic efficiency is smaller than 1. Oxygen reduction reaction, which can also participate to the self-discharge of the electrode should be minimized as much as possible for energy storage application. The presence of oxygen can lead to the degradation of the electrode through corrosion process, as it seems to be the case for VN thin film electrodes. Consequently, all further experiments were conducted under nitrogen bubbling of the electrolyte in a closed cell.

Determination of a suitable lower potential limit.—Figure 6a presents the different cyclic voltammograms obtained between the OCP (−0.65 V) and various more negative potential limit values for the same electrode. The CV is still rectangular in shape down to a negative potential limit of −1.1 V, but a large irreversible cathodic current is measured for potentials more negative than −1.1 V, introducing a slight decrease of the Coulombic efficiency (94%). This current is most likely attributed to the irreversible hydrogen evolution reaction (Eq. 2).

$$H_2O + 2e^- \leftrightarrows H_2 + 2OH^- \qquad [2]$$

Similarly to the oxygen reduction reaction, the charge consumed by this reaction is not recovered upon oxidation and is obviously not useful for energy storage. Again, for the same reason, it could also hide or minimize the presence of an unwanted irreversible anodic reaction, when the Coulombic efficiency is considered. Moreover, even if this reaction is known for its slow kinetics on some electrode material, it will lead to self-discharge until its potential reaches the equilibrium potential of the reaction for this particular electrode/electrolyte couple ($E^\circ = -0.931$ V vs. Hg/HgO (1 M KOH)). At last, considering the products of reaction, long term cycling experiments in a closed cell could result in a pressure build up and a change of the electrolyte pH.

The cyclic voltammograms and the anodic to cathodic charge ratio (Qa/Qc) recorded for negative potential limits down to −1.1 V seems to suggest that the hydrogen evolution reaction (HER) is not occurring at −1.1 V. Hence, electrolytic decomposition can be possibly avoided at VN electrode by arbitrarily restricting the negative potential limit to value more positive than −0.95 V.[40] However, depending on the kinetics of the HER the data of Figure 6a alone might be insufficient to rule out the possibility that such reaction is taking place at this potential. Recently, Wu et al. showed that in situation where cyclic voltammetric and galvanostatic cycling experiments would suggest that a system has a capacitive behavior, electrochemical impedance spectroscopy proved to be useful to clearly determine the actual potential range over which true capacitive behavior is kept.[68] Figures 6b and 6c present the Nyquist and phase angle vs. frequency plots, respectively of electrochemical impedance spectroscopy (EIS) measurements performed at different negative potential limits that were used in the cyclic voltammetric experiments (Figure 6a). When the electrode potential is more positive than −1.0 V a capacitive behavior, demonstrated by an almost vertical line (Figure 6b) and a phase angle of −80° at lower frequencies (Figure 6c), is observed. The decrease of the imaginary impedance at 10 mHz when the potential is changed from −0.8 to −1.0 V indicates a slight increase of the capacitance in agreement with the cyclic voltammetric data (Figure 6a). However, a drastic change in behavior is observed when the VN thin film electrode is polarized at potential more negative than −1.0 V. Indeed the Nyquist plot for a potential of −1.1 V presents a large semi-circle characteristic of a charge transfer process (Figure 6b). Moreover, the decrease of the diameter of the semi-circle for a potential of −1.2 V indicates a decrease of the charge transfer resistance of an electrochemical reaction. The most likely electrochemical process is the hydrogen evolution reaction that is taking place at the VN/1 M KOH interface. Figure 6c further confirms that the electrode is losing its capacitive behavior when the potential is more negative than −1.0 V. The CV and EIS data allow concluding that a negative potential limit of −1.0 V should be used when cycling a VN thin film electrode in 1 M KOH.

Determination of a suitable upper potential limit.—The procedure used to determine the lower potential limit was also adopted to determine the positive potential limit. Figure 7a presents the cyclic

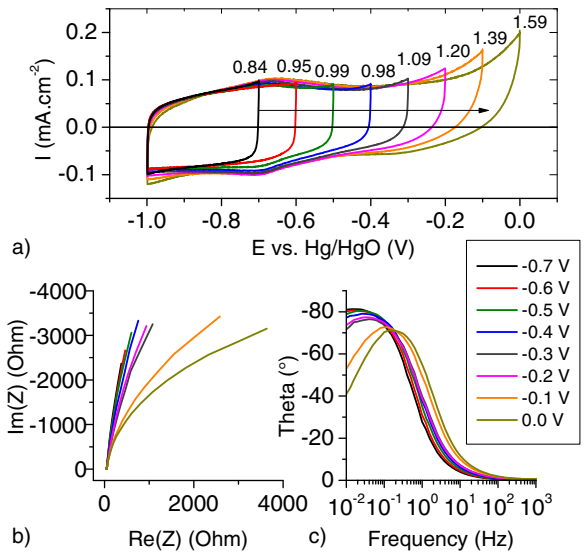

Figure 7. a) Cyclic voltammograms of VN thin film electrode between −1.0 V and various more positive potential limits (from −0.7 to 0 V). The values at each upper potential limit represent the ratio of anodic and cathodic charge (Qa/Qc). b) Nyquist plots (1 kHz - 10 mHz) and c) Bode plots measured by electrochemical impedance spectroscopy at these various negative potential limits. Measurements made in 1 M KOH under N_2 atmosphere.

voltammograms obtained between −1.0 V and different positive potential limits for the same electrode. When cycled up to 0 V, a clear irreversible anodic process can be identified. The increase of the Qa/Qc ratio to value higher than 1 for each potential window where the upper limit is more positive than −0.3 V is indicative of an irreversible anodic process. Moreover, currents recorded at a specific potential are different from one cycle to another. For example, currents recorded at −0.2 V for cycles with upper reversal potential of −0.2, −0.1 and 0 V diminish from one cycle to another even though currents recorded at −0.7 V are quite similar for the same cycles. This observation suggests a passivation or at least a change in the film surface composition. This is further confirmed by the appearance of an irreversible cathodic current between −0.9 and −1.0 V for reversal potential more positive than −0.3 V. However, the intensity of current of the redox peaks, centered at around 0.67 V depends on the positive potential limit when it is varied between −0.6 and −0.3 V.

EIS measurements presented in Figures 7b and 7c show an obvious deviation from a capacitive behavior for potentials more positive than −0.1 V as demonstrated by a decrease of the phase angle at low frequency. This observation suggests the occurrence of an anodic reaction such as an oxidation of the VN surface. The slow decrease of the width of the semi-circle radius observed in Figure 7b when the potential is more positive suggests a redox reaction with sluggish kinetics (large charge transfer resistance). This could however explain why in most charge/discharge cycling experiments reported in the literature, a positive potential limit of 0 V is used and that irreversible anodic processes are only observed at low cycling rate.[40–43] However, small deviation from the capacitive behavior can already be seen for potential as low as −0.5 V (Figure 7c). It is then difficult to determine from those EIS measurements which positive potential limit should be chosen in order to ensure long cycle life for the VN thin film electrode.

Afterwards, the long-term cycling stability of VN thin films was investigated over different potential windows. Figures 8a and 8b present the evolution of capacitance over 1000 cycles carried out at 20 mV.s^{-1} in between −1.0 V and 3 selected positive potential limits (−0.5, −0.4 and −0.3 V). A general loss of capacitance was observed over the first 400 cycles irrespective of the potential window (Figure 8a). When cycled up to −0.4 or −0.5 V, the capacitance stabilized after 400 cycles, leading to 88% capacity retention after 1000 cycles. However, when cycled up to −0.3 V, Figures 8a and 8b exhibit a continuous capacitance loss between the 300th and the 1000th cycle with a capacity retention of only 72% after 1000 cycles. The linear behavior of this capacitance fade suggests that a continuous dissolution or passivation is taking place at the VN electrode every time its potential is more positive than −0.4 V. The general decrease in current density observed on the cyclic voltammograms further corroborates this hypothesis (inset Figure 8b). Analogously, oxidation and formation of soluble vanadium hydroxides have been suggested to explain fast capacitance loss when the potential limit extended towards too positive potentials.[45,58] Cycling a VN electrode by using a positive potential limit of −0.5 or −0.4 V yields the same capacitance retention (Figure 8b). However, thin films cycled between −1.0 and −0.4 V showed a 4 mF.cm^{-2} capacitance enhancement due to an increase of the contribution of the redox peaks (≈ −0.67 V, see insets Figure 8a). From these different observations, potential cycling between −1.0 and −0.4 V appears to be the best conditions to obtain a good stability and high capacitance in a 1 M KOH electrolyte.

Cycling stability.—To further investigate the cycling stability, the VN thin film was tested for 10000 cycles between −1.0 and −0.4 V in 1 M KOH. Figure 9 shows that cycling in these conditions allowed the electrode to keep 74% of its initial capacitance. However, a significant loss (13%) of capacitance takes place during the first 500 cycles. This loss can either be due to either a degradation process that occurred upon the first 500 cycles, or a process that took place once the VN thin film was in presence of the electrolyte. In order to discriminate between these two hypotheses, the capacitance evolution of an electrode cycled after being kept in the electrolyte for 24 hours is also presented in Figure 9. This electrode shows a smaller

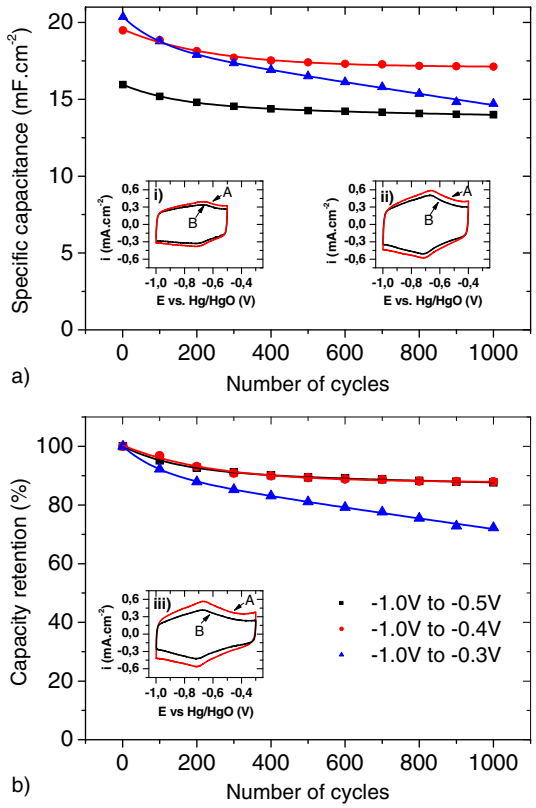

Figure 8. a) Specific capacitance and b) relative capacity retention over 1000 cyclic voltammetry cycles at 20 mV.s^{-1} in between −1.0 V and three different upper limits: −0.5 (■), −0.4 (●) and −0.3 V (▲). The insets present the first (A) and 1000th (B) cyclic voltammograms obtained for different potential windows (from left to right, (i- [−1.0; −0.5]; ii- [−1.0; −0.4] and iii- [−1.0; −0.3] V).

initial capacitance compared to the former electrode. This observation suggests that the capacitance loss observed over the first 500 cycles, when the electrode is cycled without any prior stabilization time, is probably due to a process taking place when the electrode is in presence of 1 M KOH, whether the electrode is cycled or not. One can suspect the presence of an unstable surface oxide that contributes to the charge storage process. The dissolution of this surface oxide in the 1 M KOH electrolyte would then lead to a capacitance loss. However, further experiments are needed to validate this hypothesis. In these experimental conditions, which are a constant nitrogen bubbling in the 1 M KOH electrolyte, a 24 hours resting period prior to cycling and an

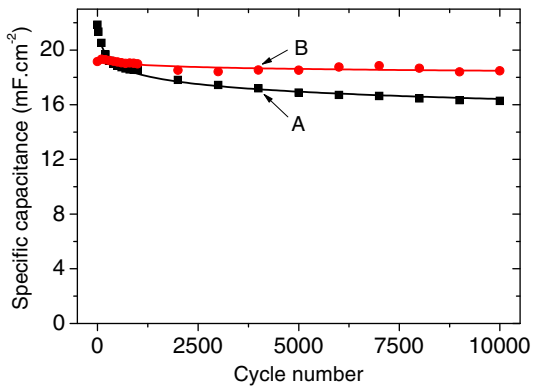

Figure 9. Specific capacitance over 10000 cyclic voltammetry cycles at 20 mV.s^{-1} in 1 M KOH between −1.0 and −0.4 V, immediately after being exposed to the electrolyte (curve A) and after a stabilization time of 24 h (curve B), prior to cycling.

optimized potential window ([−1.0; −0,4] V), an impressive capacity retention of 96% was achieved over 10000 cycles.

Conclusions

This study has clearly demonstrated that VN is active for the oxygen reduction reaction and the presence of oxygen in the electrolyte should be avoided as well as the negative potential excursion should be limited in such a way to avoid the hydrogen evolution reaction. Moreover, in order to maintain a long cycle life, a VN thin film electrode should not be cycled to potential more positive than −0.4 V. As a result, cycling a VN thin film electrode between −1.0 and −0.4 V in 1 M KOH electrolyte after a prior 24 hours stabilization period resulted in an initial capacitance of 19 mF.cm^{-2} with a capacity retention of 96% after 10000 cycles. It is worth noting that such performance combined with the simple and reproducible PVD synthesis of VN thin films make them attractive for electrochemical microsupercapacitor applications.[46,47,69,70]

The VN pseudocapacitive behavior is thought to be due to surface oxide redox processes.[58] This has been further supported by surface characterization following cycling experiment between 0.0 and −1.2 V.[41,58] However, the fact that the VN was found to be unstable in 1 M KOH for potential more positive than −0.4 V demonstrates that further investigation is needed to confirm that the observed surface oxide was not just the result of some oxidation/degradation process. Additionally, in this study, the presence of oxygen was shown to shift the open circuit potential of a VN electrode to about 0 V by self-discharge. Consequently, in order to make sure that ex-situ characterization measurements are representative of the real state of the material in the electrolyte, characterization of the surface composition after cycling should be performed without exposing the VN electrode to ambient air.

Acknowledgments

The financial supports of the Natural Science and Engineering Research Council of Canada (NSERC) as well as the French Ministry of Education, Research and Technologie are gratefully acknowledged. Ecole Polytechnique de Montréal (cm^2), NanoQAM and CQMF are also acknowledged.

References

1. A. G. Pandolfo and A. F. Hollenkamp, *J. Power Sources*, **157**, 11 (2006).
2. J. Chmiola, G. Yushin, Y. Gogotsi, C. Portet, P. Simon, and P. L. Taberna, *Science*, **313**, 1760 (2006).
3. C. Largeot, C. Portet, J. Chmiola, P. Taberna, Y. Gogotsi, and P. Simon, *J. Am. Chem. Soc.*, **130**, 2730 (2008).
4. S. A. Al-Muhtaseb and J. A. Ritter, *Adv. Mater.*, **15**, 101 (2003).
5. M. Sevilla, S. Álvarez, T. A. Centeno, A. B. Fuertes, and F. Stoeckli, *Electrochim. Acta*, **52**, 3207 (2007).
6. D. N. Futaba, K. Hata, T. Yamada, T. Hiraoka, Y. Hayamizu, Y. Kakudate, O. Tanaike, H. Hatori, M. Yumura, and S. Iijima, *Nat. Mater.*, **5**, 987 (2006).
7. S. Talapatra, S. Kar, S. K. Pal, R. Vajtai, L. Ci, P. Victor, M. M. Shaijumon, S. Kaur, O. Nalamasu, and P. M. Ajayan, *Nat. Nanotechnol.*, **1**, 112 (2006).
8. Y. Gogotsi, A. Nikitin, H. Ye, W. Zhou, J. E. Fischer, B. Yi, H. C. Foley, and M. W. Barsoum, *Nat. Mater.*, **2**, 591 (2003).
9. D. Bélanger, X. Ren, J. Davey, F. Uribe, and S. Gottesfeld, *J. Electrochem. Soc.*, **147**, 2923 (2000).
10. C. K. Chiang, C. R. Fincher, Y. W. Park, A. J. Heeger, H. Shirakawa, E. J. Louis, S. C. Gau, and A. G. MacDiarmid, *Phys. Rev. Lett. Lett.*, **39**, 1098 (1977).
11. M. Mastragostino, C. Arbizzani, R. Paraventi, and A. Zanelli, *J. Electrochem. Soc.*, **147**, 407 (2000).
12. A. Rudge, J. Davey, I. Raistrick, S. Gottesfeld, and J. P. Ferraris, *J. Power Sources*, **47**, 89 (1994).
13. T. Brousse, D. Belanger, and J. W. Long, *J. Electrochem. Soc.*, **162**, A5185 (2015).
14. B. E. Conway, *Electrochemical Supercapacitors: Scientific Fundamentals and Technological Applications*; Kluwer, 1999.
15. S. Trasatti and G. Buzzanca, *J. Electroanal. Chem.*, **29**, A1 (1971).
16. R. Fu, Z. Ma, and J. P. Zheng, *J. Phys. Chem. B*, **106**, 3592 (2002).
17. W. Dmowski, T. Egami, K. E. Swider-lyons, C. T. L. Love, and D. R. Rolison, *J. Phys. Chem. B*, **106**, 12677 (2002).
18. T. Lui, W. G. Pell, and B. E. Conway, *Electrochim. Acta*, **42**, 3541 (1997).
19. H. Y. Lee and J. B. Goodenough, *J. Solid State Chem.*, **148**, 81 (1999).
20. M. Toupin, T. Brousse, and D. Belanger, *Chem. Mater.*, **16**, 3184 (2004).
21. T. Brousse, M. Toupin, R. Dugas, L. Athouel, O. Crosnier, and D. Bélanger, *J. Electrochem. Soc.*, **153**, A2171 (2006).
22. D. Bélanger, T. Brousse, and J. W. Long, *Electrochem. Soc. interface*, 49 (2008).
23. S. Devaraj and N. Munichandraiah, *J. Phys. Chem. C*, **112**, 4406 (2008).
24. O. Ghodbane, J.-L. Pascal, and F. Favier, *ACS Appl. Mater. Interfaces*, **1**, 1130 (2009).
25. J. P. Zheng, P. J. Cygan, and T. R. Jow, *J. Electrochem. Soc.*, **142**, 2699 (1995).
26. K. E. Swider-Lyons, C. T. Love, and D. R. Rolison, *J. Electrochem. Soc.*, **152**, C158 (2005).
27. K.-H. Chang and C.-C. Hu, *J. Electrochem. Soc.*, **151**, A958 (2004).
28. W. Sugimoto, H. Iwata, Y. Yasunaga, Y. Murakami, and Y. Takasu, *Angew. Chem. Int. Ed. Engl.*, **42**, 4092 (2003).
29. M. R. Lukatskaya, O. Mashtalir, C. E. Ren, Y. Dall'Agnese, P. Rozier, P. L. Taberna, M. Naguib, P. Simon, M. W. Barsoum, and Y. Gogotsi, *Science*, **341**, 1502 (2013).
30. Y. Dall'Agnese, M. R. Lukatskaya, K. M. Cook, P.-L. Taberna, Y. Gogotsi, and P. Simon, *Electrochem. Commun.*, **48**, 118 (2014).
31. M. Wixom, L. Owens, J. Parker, J. Lee, I. Song, and L. Thompson, *Electrochem. Soc. Proc.*, **96-25**, 63 (1997).
32. L. Owens, L. T. Thompson, and M. R. Wixom, High surface area mesoporous desigel materials and methods for their fabrication. US Patent 5837630, 1998.
33. C. Z. Deng and K. C. Tsai, *Electrochem. Soc. Proc.*, **96-25**, 75 (1997).
34. D. A. Evans and J. R. Miller Capacitor including a cathode having a nitride coating. US patent 5754394, 1998.
35. L. T. Thompson, M. R. Wixom, and J. M. Parker, High surface area nitride, carbide and boride electrodes and methods of fabrication thereof. US Patent 5680292, 1997.
36. D. Choi and P. N. Kumta, 2298 (2006).
37. D. Choi and P. N. Kumta, *Electrochem. Solid-State Lett.*, **8**, A418 (2005).
38. S. L. Roberson, D. Finello, and R. F. Davis, *J. Appl. Electrochem.*, **29**, 75 (1999).
39. T.-C. Liu, W. G. Pell, and B. E. Conway, *J. Electrochem. Soc.*, **145**, 1882 (1998).
40. X. Zhou, H. Chen, D. Shu, C. He, and J. Nan, *J. Phys. Chem. Solids*, **70**, 495 (2009).
41. D. Shu, C. Lv, F. Cheng, C. He, K. Yang, J. Nan, and L. Long, *Int. J. Electrochem. Sci.*, **8**, 1209 (2013).
42. A. M. Glushenkov, D. Hulicova-jurcakova, D. Llewellyn, G. Q. Lu, and Y. Chen, *Chem. Mater.*, **22**, 914 (2010).
43. L. Zhang, C. M. B. Holt, E. J. Luber, B. C. Olsen, H. Wang, M. Danaie, X. Cui, X. W. Tan, V. Lui, W. P. Kalisvaart, and D. Mitlin, *J. Phys. Chem. C*, **115**, 24381 (2011).
44. P. Pande, P. G. Rasmussen, and L. T. Thompson, *J. Power Sources*, **207**, 212 (2012).
45. R. L. Porto, R. Frappier, J. B. Ducros, C. Aucher, H. Mosqueda, S. Chenu, B. Chavillon, F. Tessier, F. Cheviré, and T. Brousse, *Electrochim. Acta*, **82**, 257 (2012).
46. R. Lucio-Porto, S. Bouhtiyya, J. F. Pierson, A. Morel, F. Capon, P. Boulet, and T. Brousse, *Electrochim. Acta*, **141**, 203 (2014).
47. E. Eustache, R. Frappier, R. L. Porto, S. Bouhtiyya, J.-F. Pierson, and T. Brousse, *Electrochem. Commun.*, **28**, 104 (2013).
48. C. M. Ghimbeu, E. Raymundo-Piñero, P. Fioux, F. Béguin, and C. Vix-Guterl, *J. Mater. Chem.*, **21**, 13268 (2011).
49. S. Dong, X. Chen, L. Gu, X. Zhou, H. Wang, Z. Liu, P. Han, J. Yao, L. Wang, G. Cui, and L. Chen, *Mater. Res. Bull.*, **46**, 835 (2011).
50. F. Cheng, C. He, D. Shu, H. Chen, J. Zhang, S. Tang, and D. E. Finlow, *Mater. Chem. Phys.*, **131**, 268 (2011).
51. P. J. Hanumantha, M. K. Datta, K. S. Kadakia, D. H. Hong, S. J. Chung, M. C. Tam, J. A. Poston, A. Manivannan, and P. N. Kumta, *J. Electrochem. Soc.*, **160**, A2195 (2013).
52. X. Lu, T. Liu, T. Zhai, G. Wang, M. Yu, S. Xie, Y. Ling, C. Liang, Y. Tong, and Y. Li, *Adv. Energy Mater.*, **4**, 1300994 (2013).
53. Z.-H. Gao, H. Zhang, G.-P. Cao, M.-F. Han, and Y.-S. Yang, *Electrochim. Acta*, **87**, 375 (2013).
54. R. Wang, X. Yan, J. Lang, Z. Zheng, and P. Zhang, *J. Mater. Chem. A*, **2**, 12724 (2014).
55. Y. Su and I. Zhitomirsky, *J. Power Sources*, **267**, 235 (2014).
56. Y. Yang, R. Kirchgeorg, R. Hahn, and P. Schmuki, *Electrochem. Commun.*, **43**, 31 (2014).
57. M. Balogun, W. Qiu, W. Wang, P. Fang, X. Lu, and Y. Tong, *J. Mater. Chem. A*, **3**, 1364 (2015).
58. D. Choi, G. E. Blomgren, and P. N. Kumta, *Adv. Mater.*, **18**, 1178 (2006).
59. S. T. Oyama, *The chemistry of transition metal carbides and nitrides*; S. T. Oyama, Ed.; Chapman & Hall, 1996.
60. P. Krawiec, P. L. De Cola, R. Gläser, J. Weitkamp, C. Weidenthaler, and S. Kaskel, *Adv. Mater.*, **18**, 505 (2006).
61. T. Onozuka, *J. Appl. Cryst.* **11**, 132 (1978).
62. J. C. Caicedo, G. Zambrano, W. Aperador, L. Escobar-alarcon, and E. Camps, *Appl. Surf. Sci.*, **258**, 312 (2011).
63. K. Ait Aissa, A. Achour, J. Camus, L. Le Brizoual, P. Y. Jouan, and M. A. Djouadi, *Thin Solid Films*, **550**, 264 (2014).
64. B. D. Choi, G. E. Blomgren, and P. N. Kumta, 1178 (2006).
65. W.-F. Chen, J. T. Muckerman, and E. Fujita, *Chem. Commun.*, **49**, 8896 (2013).
66. C. Pozo-Gonzalo, O. Kartachova, A. A. J. Torriero, P. C. Howlett, A. M. Glushenkov, D. M. Fabijanic, Y. Chen, S. Poissonnet, and M. Forsyth, *Electrochim. Acta*, **103**, 151 (2013).
67. M. Yang, A. J. Allen, M. T. Nguyen, W. T. Ralston, M. J. MacLeod, and F. J. DiSalvo, *J. Solid State Chem.*, **205**, 49 (2013).
68. T.-H. Wu, Y.-H. Chu, C.-C. Hu, and L. J. Hardwick, *Electrochem. Commun.*, **27**, 81 (2013).
69. M. Beidaghi and Y. Gogotsi, *Energy Environ. Sci.*, **7**, 867 (2014).
70. M. Brunet and D. Pech, *Techniques de l'ingénieur* 2012, *Re210*.